

Metamorphic Runtime Monitoring of Autonomous Driving Systems

JON AYERDI, Mondragon University, Spain
 ASIER IRIARTE, Mondragon University, Spain
 PABLO VALLE, Mondragon University, Spain
 IBAI ROMAN, Mondragon University, Spain
 MIREN ILLARRAMENDI, Mondragon University, Spain
 AITOR ARRIETA, Mondragon University, Spain

Autonomous Driving Systems (ADSs) are complex Cyber-Physical Systems (CPSs) that must ensure safety even in uncertain conditions. Modern ADSs often employ Deep Neural Networks (DNNs), which may not produce correct results in every possible driving scenario. Thus, an approach to estimate the confidence of an ADS at runtime is necessary to prevent potentially dangerous situations. In this paper we propose MARMOT, an online monitoring approach for ADSs based on Metamorphic Relations (MRs), which are properties of a system that hold among multiple inputs and the corresponding outputs. Using domain-specific MRs, MARMOT estimates the uncertainty of the ADS at runtime, allowing the identification of anomalous situations that are likely to cause a faulty behavior of the ADS, such as driving off the road.

We perform an empirical assessment of MARMOT with five different MRs, using a small-scale ADS, two different circuits for training, and two additional circuits for evaluation. Our evaluation encompasses the identification of both external anomalies, e.g., fog, as well as internal anomalies, e.g., faulty DNNs due to mislabeled training data. Our results show that MARMOT can identify 35% to 65% of the external anomalies and 77% to 100% of the internal anomalies, outperforming both SelfOracle and Ensemble-based ADS monitoring approaches.

ACM Reference Format:

Jon Ayerdi, Asier Iriarte, Pablo Valle, Ibai Roman, Miren Illarramendi, and Aitor Arrieta. 2023. Metamorphic Runtime Monitoring of Autonomous Driving Systems. 1, 1 (October 2023), 20 pages. <https://doi.org/XXXXXXX.XXXXXXX>

1 INTRODUCTION

In the last few years, the autonomy of vehicles is increasing, in part, thanks to the recent advances of machine-learning based technologies. Deep Neural Networks (DNNs) have enabled Autonomous Driving Systems (ADSs) to operate in dynamic environments with little to no human intervention [8]. Supervised training is a particularly effective approach that allows DNNs to effectively learn driving behaviors (such as the throttling or the steering angle) from labeled datasets of camera images and the corresponding expected driving behavior [8]. However, to deploy ADSs in the roads, these

Authors' addresses: Jon Ayerdi, Mondragon University, Goiru 2, Mondragon, Gipuzkoa, Spain, 20500, jayerdi@mondragon.edu; Asier Iriarte, Mondragon University, Goiru 2, Mondragon, Gipuzkoa, Spain, 20500, asier.iriarte@alumni.mondragon.edu; Pablo Valle, Mondragon University, Goiru 2, Mondragon, Gipuzkoa, Spain, 20500, pablo.valle@alumni.mondragon.edu; Ibai Roman, Mondragon University, Goiru 2, Mondragon, Gipuzkoa, Spain, 20500, iroman@mondragon.edu; Miren Illarramendi, Mondragon University, Goiru 2, Mondragon, Gipuzkoa, Spain, 20500, millarramendi@mondragon.edu; Aitor Arrieta, Mondragon University, Goiru 2, Mondragon, Gipuzkoa, Spain, 20500, aarrieta@mondragon.edu.

Permission to make digital or hard copies of all or part of this work for personal or classroom use is granted without fee provided that copies are not made or distributed for profit or commercial advantage and that copies bear this notice and the full citation on the first page. Copyrights for components of this work owned by others than ACM must be honored. Abstracting with credit is permitted. To copy otherwise, or republish, to post on servers or to redistribute to lists, requires prior specific permission and/or a fee. Request permissions from permissions@acm.org.

© 2023 Association for Computing Machinery.

XXXX-XXXX/2023/10-ART \$15.00

<https://doi.org/XXXXXXX.XXXXXXX>

should be reliable, even in the presence of uncertain or unforeseen scenarios. To increase the reliability of these systems, in the last few years, significant effort has been devoted to research on automated test case generation techniques that falsify safety properties of ADSs (e.g., find collisions, violate traffic laws) [1, 2, 6, 7, 9, 14, 15, 17, 18, 30, 37, 43, 44, 51, 52]. However, the expensive execution of test cases (due to the use of simulation frameworks), as well as the huge input space, makes it impossible to cover all situations in which the ADS can misbehave.

To address this issue, existing works propose runtime monitors (also known as supervisors or failure predictors) to assess the level of the DNN dependability in operation [20, 23, 24, 39, 41, 42, 45, 47, 50]. In the context of ADSs, both, black-box as well as white-box approaches have been proposed. As for black-box approaches, techniques like SelfOracle [42] or DeepGuard [23] monitor the ADS by examining its behavior in response to the input images of the system. In the context of ADS, for black-box runtime monitoring techniques, one of the identified core limitations [39] relates to the impossibility of handling other failures than those caused due to data-driven bugs, e.g., failures caused by corrupted images. Therefore, these techniques fail to detect faults due to inadequate training or by bugs at the DNN model level [39]. To address this challenge, Stocco et al. [39] proposed ThirdEye, a white-box ADS failure predictor that relies on attention maps produced by explainable artificial intelligence (XAI) techniques. Specifically, they propose three different summarization methods to compute a confidence score from the attention map of the images, provided some extra information previously extracted from the training dataset. Although this technique is promising and overcomes the limitations of black-box techniques, it also poses one core limitation that may prevent its adoption in practice: its computational cost, and as a direct consequence, its execution time. Specifically, the techniques employed to obtain the attention maps require several invocations of the DNN, which may make this technique unfeasible unless significant computational resources are available exclusively for the ADS monitors. This may be a problem in the context of ADS that use resource-constrained embedded devices.

To deal with the above-mentioned challenges, we propose MARMOT, a simple, yet effective and efficient runtime monitoring approach. MARMOT leverages ideas from metamorphic testing [38] to predict when the ADS will fail, and it provides significant benefits over the state-of-the-art approaches. Firstly, based on our experiments with a lane keeping case study system, MARMOT provides **higher effectiveness** in terms of detecting internal (faulty DNN models) or external (unexpected inputs) anomalies which may cause an incorrect behavior of the system. Secondly, our approach is capable of an **earlier detection** of internal anomalies than other approaches, which is crucial in cases where there is only a short time to react. Furthermore, MARMOT is also applicable for ADSs whose functionalities are not necessarily controlled through DNNs, such as in the case of Apollo [3]. Lastly, our approach only requires cheap image transformations and one additional invocation of the ADS controller (either DNN or other), which would solve the high computational cost of some white-box techniques (e.g., ThirdEye [39]).

Our paper makes the following contributions:

- **Technique:** We propose a black-box approach inspired on Metamorphic Testing to estimate the confidence of DNN-based ADSs at runtime. We define several image-based Metamorphic Relations (MRs) for this domain, and a process to evaluate them at runtime. Our technique can be used to identify potentially unexpected scenarios, either those derived from internal (e.g., improperly trained DNN) or external (e.g., fog blocking the visibility of the camera) uncertainties.
- **Evaluation:** Unlike previous studies, which use simulation environments in their evaluation, we employ a physical (small-scale) ADS. This was considered to reduce the validity threat related to the reality gap existing between simulated and real environments (e.g., due to the

textures of the images or the fidelity of the simulation engines). With this physical vehicle, we carry out an empirical study, showing MARMOT's benefits over the black-box approach of SelfOracle [42] as well as the white-box Ensemble approach.

- **Dataset:** We provide the dataset of images used to train our DNN-based driving models, as well as the one used to evaluate our test oracles in this paper [4]. Our dataset comprises images from a training track provided by the vendor of the mobile robot [27], as well as images from another training track and two additional evaluation tracks provided by us. For the two evaluation tracks, our dataset also includes recordings of out-of-bounds scenarios, caused by either internal (faulty DNN models) or external (unexpected inputs) anomalies.

The rest of the paper is structured as follows: We provide basic background in Section 2. We explain our approach in Section 3. We empirically evaluate our approach in Section 4, by means of a physical small-scale autonomous driving systems and different types of anomalies. We position our approach with the current state-of-the-art in Section 5. Lastly, we conclude and discuss future research avenues in Section 6.

2 BACKGROUND

2.1 Autonomous Driving Systems

Modern Autonomous Driving Systems (ADSs) leverage machine-learning technologies, such as Deep Neural Networks (DNN), to analyze the inputs (e.g., camera images, LIDAR sensors, GPS) and drive the vehicle in real time with various degrees of autonomy [8]. Typically, DNNs learn tasks such as lane keeping in a supervised manner, i.e., by generalizing from a dataset of samples labeled by humans, which demonstrate correct driving behaviors [8].

However, DNN-based driving systems are currently unlikely to generalize correctly for all possible driving conditions that can be encountered in a real road. Thus, in order to ensure safety, it is paramount to monitor the (estimated) confidence of the DNN, so that an appropriate healing strategy can be applied in low-confidence scenarios. Healing strategies to leave the vehicle in a safe state may include passing control to a human driver, reducing the speed, or completely stopping the vehicle [23].

2.2 Monitoring Techniques for ADSs

An approach to monitor a DNN's behaviour and quantify its confidence level must consider several causes of uncertainty. On the one hand, this includes external factors, such as adverse environmental conditions like fog or heavy rain [23, 42, 44]. On the other hand, internal factors such as poorly trained DNNs (e.g., wrong hyperparameter values, incorrect labels in the training dataset) may also need to be considered [21, 39].

Black-box techniques estimate the confidence of the DNN based solely on its inputs (images) and outputs (steering angle, throttle, etc.), and possibly also the training data [42]. The main advantage of these techniques is that they are independent from the DNN architecture, and often even generalizable to systems which do not even employ DNNs. Nevertheless, their lack of knowledge of the DNNs internal behavior might limit the ability of these techniques to react to internal uncertainties [39]. A popular black-box approach for estimating the confidence of DNNs in the context of ADSs is using autoencoders, which are DNNs that can reconstruct an input image, to identify inputs beyond the distribution of the inputs with which the ADS has been trained [23, 42]. Metamorphic testing is an alternative black-box technique that can be used to identify inconsistencies in an ADS without interacting with its internals [44, 50].

Conversely, white-box techniques monitor the internal behavior of the DNN, require a transparent access to the network, and are often specifically designed for networks with specific features.

However, the knowledge of the DNN's internal behavior may allow these techniques to identify internal uncertainties that black-box techniques cannot. For example, with Deep Ensemble Neural Networks, multiple DNN models with different weight initialization or hyperparameters are trained with the same dataset to obtain a probability distribution of the model output [26]. This distribution can then be used to infer the confidence of the DNN for the corresponding inputs [26].

2.3 Metamorphic Testing

Metamorphic Testing (MT) is an alternative technique to alleviate the test oracle problem that exploits known input and output relations that should hold among *multiple* test executions, the so-called Metamorphic Relations (MRs) [10]. As an example, if the input image for an image-based classifier DNN is altered by slightly increasing its brightness, the output of the DNN should remain almost unchanged. Here, the MR we define consists of an *Input Relation* (IR) ($img_2 = \text{brighten}(img_1)$) and an *Output Relation* (OR) ($output_2 \approx output_1$).

Typically, MT is performed with pairs of test cases: A *source* test case, which is usually generated by a test generation strategy (e.g., random test generation), and a *follow-up* test case, generated by *transforming* the source test case in a way that the input relation of the MR is satisfied [10, 38]. For the given example, the follow-up image can be generated by brightening the source image. A violation of this MR (high deviation of the output between the source and follow-up images) might indicate that the DNN is not operating reliably, possibly due to uncertain conditions [46].

This technique has already been applied in various forms for testing CPSs, such as autonomous drones [29] and driverless cars [53], including DNN-based autonomous driving systems [44, 50]. Nevertheless, the existing research of this technique focuses on testing, as opposed to other verification tasks such as the online monitoring of systems.

3 APPROACH

In this paper we propose MARMOT, a metamorphic runtime monitoring technique for ADS. We specifically focus on the use of this technique to provide a DNN supervisor. This supervisor provides an uncertainty score for the system at run-time, enabling the real-time detection of misbehaviors via MRs in order to take corrective actions when these occur.

3.1 Architecture

Figure 1 shows an overview of the architecture of MARMOT, which we use for applying Metamorphic Runtime Monitoring to an ADS controlled by an image-based DNN. The top half of the image shows the three main components of the ADS: (1) the camera, for the image acquisition; (2) the DNN, for decision-making based on the images; and (3) the actuator controls, which act on the steering and throttling commands provided by the DNN.

The bottom half of the image shows the Metamorphic Runtime Monitoring components and their interactions. For each MR used by our monitor, an Input Relation (IR) and its corresponding Output Relation (OR) must be defined.

Firstly, the Input Relation ① defines a transformation of the input image. In the example from Figure 1, the IR consists of flipping the image horizontally, i.e., $img_f = \text{flip}(img_s)$. By applying this transformation to the image captured by the camera (i.e., img_s), which we consider the *source* input, we generate the *follow-up* input for the MR (i.e., img_f).

After the *follow-up* image has been generated, it is executed by the DNN to obtain its output ②. This step corresponds with the execution of the follow-up test case in Metamorphic Testing, which is possible because the DNN is usually an isolated component of the ADS, with no direct dependencies on external states. It is important to note that the output of the DNN for the follow-up image is not sent to the driving commands, but instead used for monitoring purposes.

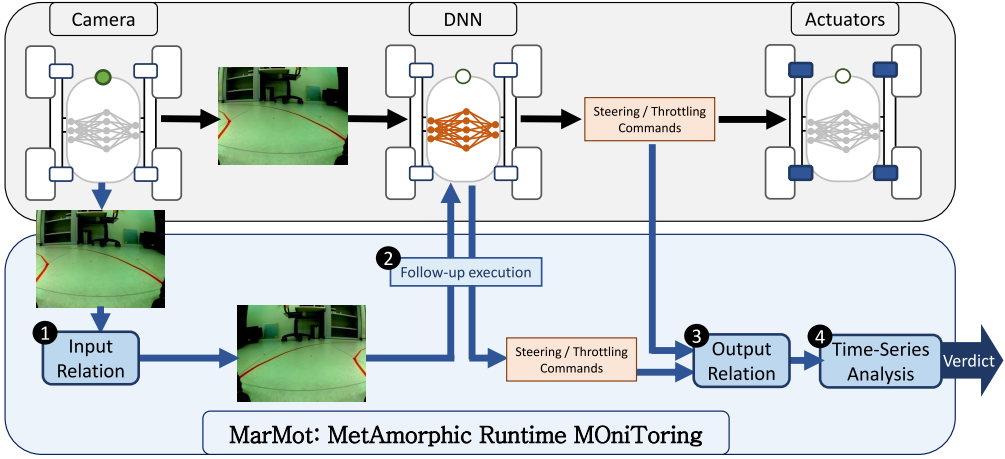


Fig. 1. Architecture of MARMot for DNN-based ADS

Finally, the Output Relation ③ defines the expected follow-up value. In the example from Figure 1, the Output Relation for the steering angle of the ADS consists of inverting the output from the source test case, i.e., $steering_f \approx -steering_s$.

To obtain an uncertainty score with this Output Relation, we emit *quantitative verdicts* based on the Euclidean distance, which is a simple way to measure the distance between the expected and actual values of the follow-up outputs:

$$u = \sqrt{(OR(O_s) - O_f)^2} \quad (1)$$

where u is the uncertainty score, $OR(O_s)$ is the expected follow-up output from the model for the follow-up image, computed with the Output Relation OR and the actual output from the model for the source image O_s , and O_f is the actual output from the model for the follow-up image.

For instance, the uncertainty score for the Output Relation described above would be computed as:

$$u = \sqrt{(-steering_s - steering_f)^2} \quad (2)$$

Under normal driving conditions in which the DNN is operating reliably, the MR is expected to hold within a certain error margin, and so the uncertainty scores are expected to remain under a certain boundary. However, unexpected situations that may make the ADS unreliable, such as environmental anomalies or inappropriate DNN training, could cause more severe MR violations, and thus increased uncertainty scores. This is why the verdicts emitted by MARMot can be interpreted as a measure of the uncertainty for the DNN. i.e., an uncertainty score.

While these quantitative verdicts can quantify the uncertainty of the DNN under test, some reference must be defined to determine whether a given value is large enough to warrant raising an alarm. A common strategy, which we employ in our implementation, is to define a threshold value based on the verdicts observed in nominal driving conditions, such as in (a subset of) the training data for the DNN.

The uncertainty score computed by an MR may be susceptible to short-term increases for a few frames, which may not be desirable to interpret as an anomalous scenario or system misbehavior. Thus, similar to SelfOracle [42], we implement a time-series based analysis ④ in order to smooth uncertainty score spikes and avoid false alarms due to single-frame outliers. Specifically, we

implement a simple auto-regressive (AR) filter that computes the uncertainty score as a linear combination of past values. The following equation describes the computation of the uncertainty score u_t at time t using the last k values:

$$u_t = \sum_{i=1}^k \frac{1}{i} u_{t-i} \quad (3)$$

3.2 Metamorphic Relations

We define five specific MRs for image-based ADSs, which we have implemented on top of MARMOT. The first four MRs define image transformations that are expected to not change the output from the DNN under normal conditions, whereas MR5 defines a transformation which should result in a symmetric steering angle as the output from the DNN. While our approach is generic to any kind of MRs for image-based ADSs, it is important to use MRs that are computationally cheap. We therefore used five MRs below, and avoid using others that are computationally more time consuming, such as frosting the image.

- **MR1: Reduce Brightness.** This transformation consists of slightly reducing the brightness of the input image. This brightness reduction has been tuned to be well within the tolerance of the DNN. Thus, the output is expected to be very similar to the original image.
- **MR2: Increase Contrast.** This transformation consists of slightly increasing the contrast of the input image. This contrast increase has been tuned to be well within the tolerance of the DNN, so the output is expected to be very similar to the original image.
- **MR3: Add Noise.** This transformation consists of slightly altering the values from individual pixels of the image, with a uniform distribution for the degree of change. The degree of the alterations has been tuned to be well within the tolerance of the DNN. Thus, the output is expected to be very similar from the original image.
- **MR4: Blur.** This transformation consists of slightly blurring the image. The degree of blurring has been tuned to be well within the tolerance of the DNN. Thus, the output is expected to be very similar to the original image.
- **MR5: Horizontal Flip.** This transformation consists of horizontally flipping (i.e., mirroring) the image, as shown in the example from Figure 1. The output from the DNN is expected to be mirrored (i.e., negated) from the one obtained with the original image.

4 EVALUATION

This section describes our empirical evaluation and presents the results obtained from our experiments. Specifically, we aim at answering the following research questions (RQs):

- RQ1 Effectiveness** – How effective is MARMOT at predicting failures of ADSs derived from internal or external anomalies? Which are the best MRs?
- RQ2 Comparison** – How does MARMOT compare with other state-of-the-art failure predictors?
- RQ3 Reaction** – How do the results for MARMOT and other state-of-the-art failure predictors change as we reduce the reaction window?

4.1 Case Study System

We evaluate MARMOT on a physical environment, using the LeoRover [28] vehicle controlled by an image-based DNN provided by the vendor. Unlike previous ADS monitoring approaches [23, 39, 42], we employed a physical system to avoid the threats to validity produced by the reality gap between simulated and physical ADSs. While we acknowledge that our small-scale ADS is still far from a real self-driving car, it is also important to note that obtaining a dataset of anomalies and DNN

faults with a real car under real conditions requires extensive resources and may potentially incur in ethical issues due to safety concerns. We therefore believe that our small scale ADS is a good step towards the assessment of monitoring techniques in real cars in more realistic conditions.



Fig. 2. LeoRover in Circuit-1

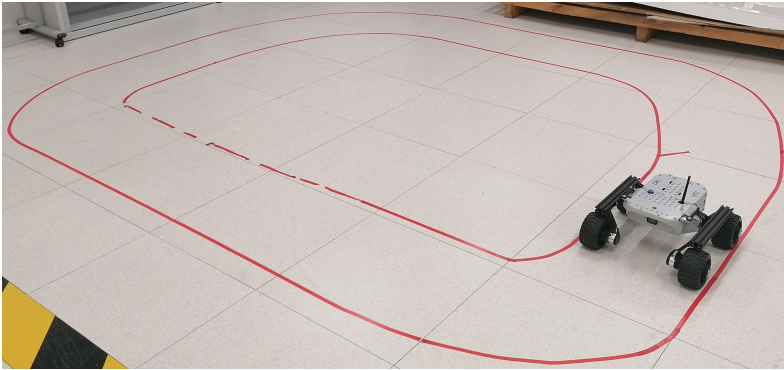


Fig. 3. LeoRover in Circuit-2

Our case study system's DNN is trained to follow a road delimited by colored tape. Figures 2 and 3 show the LeoRover vehicle driving in the two circuits we employ in our evaluation. The vehicle has a camera, which we set to record images at ~ 10 frames per second (FPSs), and four static wheels with independent motors for steering and throttling, with a maximum linear speed of ~ 0.4 m/s. The DNN model consists of five convolutional layers followed by two dense layers. The DNN was trained by ourselves for 100 epochs with a combination of the dataset provided by the vendor and an additional dataset recorded by us, which we describe in Section 4.2. The software of the LeoRover employs the Robotic Operating System (ROS) [25], and the different ADS components from Figure 1 are implemented as ROS nodes. This software architecture enables the interaction with the DNN required by MARMOT to be efficiently implemented via ROS messages.

4.2 Datasets

In this section, we describe the datasets employed to train our subject DNN and the evaluation datasets, in addition to the processes we used to collect them. To allow for a fair and reproducible empirical evaluation, we evaluated all the DNN supervisors offline. All the datasets consist of ordered lists of camera images and annotations of which frames correspond with specific events, such as out-of-bounds episodes. The images were recorded at ~ 10 FPSs, i.e., 10 images roughly

correspond with a second of recording. Each image is stored with a resolution of 120×160 and three color channels (RGB). Because we employed a physical ADS, significant manual effort was required for the collection of the dataset, lasting in total a 2 person-week effort.

4.2.1 Training Data. To train the DNN model, we combined two datasets recorded in two different circuits. The first dataset is provided by the LeoRover vendor, and consists of 10,493 labeled images. The second dataset was collected by ourselves in a test circuit, and consists of 2,832 labeled images. We extended the vendor's dataset to withstand relatively complex manoeuvres (e.g., sharp curves). The circuits we used for the training were not used for evaluation purposes later. The datasets were collected by manually driving the vehicle through the circuits with a remote controller and recording the image, throttle, and steering angle for each frame.

4.2.2 Nominal Conditions. The following datasets, which we used for the evaluation of our approach and the baselines, were collected by ourselves in two circuits, different from the ones employed for training the driving DNN. These circuits, which we named Circuit-1 and Circuit-2, can be seen in Figure 2 and Figure 3 respectively. As it can be seen in the images, Circuit-1 contains more curves and sharper turns. In comparison, Circuit-2 only contains four curves in the same direction, but we also incorporated some additional sources of environmental uncertainty (as categorized by Zhang et al. [48, 49]) in the form of discontinuous lines and an extra line inside the circuit. We verified that our DNN could successfully drive through both of these circuits under normal conditions.

To evaluate the rate of false alarms obtained with our approaches, we first collected recordings of the DNN driving in both circuits under nominal conditions, with no out-of-bounds events nor any other incidents. These recordings were arranged such that each of them corresponds roughly with one complete lap to the circuit.

Overall, for the nominal conditions dataset, we obtained a total of 37 recordings (13,416 images) for Circuit-1 and 35 recordings for Circuit-2 (8,320 images), each of which corresponds with one lap to the circuit.

4.2.3 Anomalies. To measure the ability of our DNN supervisors to identify external anomalies, we collected a dataset of out-of-bounds episodes resulting from unexpected anomalies in the images. For this purpose, we implemented the image corruptions and perturbations proposed by Hendrycks et al. [19], which are widely used for testing image-based DNNs [13, 16, 36, 40]. For our experiments, we could only use 13 out of the 19 proposed image corruptions due to performance limitations when applying the image transformations while the vehicle is running. For each of the anomalies, five different levels are employed.¹ The employed image corruptions include the following:

- Gaussian noise
- Shot noise
- Impulse noise
- Defocus blur
- Glass blur
- Fog
- Brightness
- Contrast
- Pixelate
- JPEG compression
- Speckle noise

¹The specific values for each of the anomalies can be found in https://github.com/jonayerdi/marmot/blob/master/leorover_scripts/hendrycks.py

- Gaussian blur
- Spatter
- Saturation

To emulate the occurrence of these external anomalies, we modified the DNN script to apply the image transformation to every image to be processed by the DNN, starting after 20 seconds from the moment the first image is processed. Therefore, each recording for external anomalies consists of ~20 seconds of normal driving conditions, followed by a window of anomalous external conditions which lasts until the out-of-bounds occurs. The frames in which the anomalous external conditions begin and the out-of-bounds occurs were annotated for each recording by manually inspecting the images.

Overall, for the external uncertainties dataset, we obtained a total of 52 recordings (13,948 images) for Circuit-1 and other 52 recordings for Circuit-2 (12,963 images), each of which ends with an out-of-bounds episode after an image perturbation is applied. Specifically, we have 13 types of anomalies, with 2 severity parameterizations for each anomaly, and we collect 2 recordings for each anomaly type and parameterization, hence $13 \times 2 \times 2 = 52$ recordings for each circuit.

4.2.4 Mutants. To measure the ability of our DNN supervisors to identify internal anomalies, we collected a dataset of out-of-bounds episodes caused by faulty driving models. For this purpose, we implemented the mutation operators for DNNs proposed by Humatova et al. [22], which are based on real deep learning faults. These mutation operators include inadequate training data and sub-optimal choice of the model's architecture or of the training hyper-parameters [22].

Specifically, we implemented three different mutation operators that, according to the evaluation carried out in the original paper [22], were not in the group of non-killable mutants, they did not have a high triviality score and they did not produce redundant mutants. The first operator, HLR, changes the learning rate. We used two different parameterizations for this mutation, with learning rate values of 0.0001 and 0.01 (the original learning rate was 0.001). The second operator, TAN, introduces low-quality training data by adding noise to a percentage of pixels. We used two different parameterizations for this mutation, changing 15% and 25% of the pixels from the images. Lastly, TCL, changes labels of training data, mimicking wrong labeling situations. Again for this case, two different parameterizations were used, assigning a random value to the steering angle of the vehicle to 15% and 20% of the images. For each mutant and parameterization, we train 10 different models, since the mutants are stochastic [22].

For this dataset, we collected recordings of the mutant DNNs driving through the circuits until an out-of-bounds episode occurred. The frames in which the out-of-bounds occur were annotated for each recording by manually inspecting the images.

Overall, for the internal uncertainties dataset, we obtained a total of 30 recordings (13,339 images) for Circuit-1 and other 30 recordings for Circuit-2 (6,689 images), each of which ends with an out-of-bounds episode. Specifically, we used three types of mutations, with two parameterizations for each mutation, and we collected five recordings for each mutant type and parameterization, hence $3 \times 2 \times 5 = 30$ recordings for each circuit.

4.3 Baselines

4.3.1 SelfOracle. To evaluate the effectiveness of MARMOT, we compared the obtained results with SelfOracle [42], a state-of-the-art misbehaviour prediction technique based on input image reconstruction models. SelfOracle [42] estimates the confidence for the DNN based on the reconstruction error of the driving model's input images. During training, an autoencoder model is trained with the same images used to train the subject DNN. At runtime, the input images are reconstructed by the autoencoder model, and the uncertainty score is measured as the reconstruction error.

$$u = \frac{1}{WHC} \sum_{i=1, j=1, c=1}^{W, H, C} (x[c][i, j] - x'[c][i, j])^2 \quad (4)$$

where u is the uncertainty score, x_t is the input image, x' is the image reconstructed by the autoencoder from x , and W, H, C are the pixel-wise width, height, and channels of the input images. The rationale behind this is that images with a high reconstruction error may be out of the distribution from the training data, and therefore, the DNNs behavior may be unreliable for those inputs.

We specifically employed 4 different autoencoder models implemented in their open-source release² for our experiments, namely: (1) SAE (simple autoencoder with a single hidden layer), (2) DAE (deep autoencoder with five fully-connected layers), (3) CAE (convolutional autoencoder with alternating convolutional and max-pooling layers), and (4) VAE (variational autoencoder). We could not train the LSTM variant due to the limited availability of computational resources. Note, however, that the VAE was the best configuration of SelfOracle [42], and was also used in other similar evaluations [23, 39].

These autoencoder models have been trained with the images from the datasets used to train the driving model, since this is the approach that would most likely be used if SelfOracle was to be adopted in practice.

4.3.2 Ensemble. Furthermore, we also employed a simple monitor based on Deep Ensemble Neural Networks [26] as an additional baseline. Our Ensemble monitor employs 10 driving DNNs trained with different weight initializations and training/validation splits of the dataset, but the same hyperparameters. The uncertainty score for this monitor is then computed as the standard deviation of the outputs from the individual driving models for each input image.

4.4 Configuration

4.4.1 Thresholds. As mentioned at the end of Section 3.1, the uncertainty scores produced by MARMOT require a threshold value to determine whether the uncertainty score indicates normal conditions or is too high and an alarm needs to be triggered. For this purpose, we isolated 7 out of the 37 recordings of nominal driving conditions from Circuit-1, which correspond with 7 laps to the circuit. These 7 recordings were used as a reference to determine the threshold value for each of our oracles, using the following formula:

$$t_o = \max (\max (u_o(f) \forall f \in R) \forall R \in D) \cdot 1.1 \quad (5)$$

where t_o is the threshold for the oracle o , $\max (u_o(f) \forall f \in R)$ is the maximum uncertainty score obtained with the oracle o from all the frames f in recording R , and D is the set of all recordings used to compute the thresholds. We chose to add a margin of 10% for computing the threshold in order to avoid false alarms, hence the 1.1 multiplier. We consider that the oracle o raises an alarm at any point when its uncertainty score is greater than t_o .

We considered individual MRs from MARMOT and individual autoencoder models from SelfOracle to be distinct oracles, so we computed thresholds for each of them separately.

We discarded the recordings used for computing these thresholds from our evaluation dataset. Thus, our evaluation dataset for nominal conditions consists of 30 recordings from Circuit-1 and all the 35 recordings from Circuit-2.

²<https://github.com/testingautomated-usi/selforacle>

4.4.2 Time-Series Analysis. For all oracles, we applied the simple auto-regressive filter described in Section 3 using the last 10 images ($k = 10$). Note that the implementation of this filter is equivalent to the one proposed in SelfOracle [42], so we do not deviate from their proposed approach.

4.4.3 MARMOT. We used the following parameters for the implementation of our MRs. We ensured that the follow-up inputs generated with the selected MR parameters followed the input validity of the domain as defined by Riccio and Tonella [35].

- *MR1: Reduce Brightness.* We subtract 77 from the values of each pixel (saturating subtraction, so values remain between 0 and 255).
- *MR2: Increase Contrast.* We convert the image to HSV format and set the saturation value of every pixel to 50 (possible values range from 0 to 255).
- *MR3: Add Noise.* We alter the values of each pixel by a rate from 0% to 20% (uniformly sampled random value per pixel).
- *MR4: Blur.* We apply a normalized box filter, as implemented by OpenCV-Python's `cv2.blur` function, using a kernel size of 1×5 .

4.4.4 SelfOracle. For training the SelfOracle autoencoder models, image augmentation was applied using flipping, translation, shadowing, and brightness changes. 60% of the data was augmented through these transformations, matching the configuration used by Stocco et al. [42]. It is noteworthy that this algorithm is also employed in DeepGuard [23].

Due to the stochastic nature of training these autoencoder models, we trained each model 10 times with different random seeds, which affects the initialization and the image augmentations applied. All the results for SelfOracle reported in Section 4.6 are average values for the 10 models of each autoencoder type.

4.4.5 Ensemble. As mentioned in Section 4.3.2, the Ensemble oracle employs 10 different driving DNNs trained with different initializations. For each of the mutations of the driving DNN employed for our internal uncertainties dataset, we also trained 10 models with different initializations, and the Ensemble oracle employs the corresponding mutants of the driving models when evaluating the internal uncertainties dataset.

4.5 Evaluation Metrics

For each recording described in Section 4.2, a test oracle may or may not raise an alarm if its uncertainty score is greater than its threshold (Section 4.4.1). For each recording from the nominal conditions dataset, we define an instance where an alarm is raised as a false positive (*FP*), and an instance where it is not as a true negative (*TN*). Conversely, for each recording from the internal or external anomalies datasets, we define an instance where an alarm is raised as a true positive (*TP*), and an instance where it is not as a false negative (*FN*).

In our evaluation, we only considered whether an oracle fired an alarm or not for each recording, since we assumed that the alarms might cause a response and consecutive alarms will have no effect. Therefore, every individual recording described in Section 4.2 will count as exactly one *FP* or *TN* (nominal conditions dataset), or one *TP* or *FN* (anomalies or mutants datasets).

Similar to most evaluations using classifiers, we also report the false positive rate ($FPR = \frac{FP}{FP+TN}$) for the nominal conditions dataset, as well as the precision ($Prec. = \frac{TP}{TP+FP}$), the recall or true positive rate ($TPR = \frac{TP}{TP+FN}$), and the F1-score ($F1 = 2 \cdot \frac{Prec. \cdot TPR}{Prec. + TPR}$) for the anomalies datasets.

Similar to [42], we also report two threshold-independent metrics for evaluating classifiers: AUC-ROC (area under the curve of the Receiver Operating Characteristics) and AUC-PRC (area under the Precision-Recall Curve).

4.6 Analysis of the Results and Discussion

4.6.1 RQ1 – Effectiveness. Table 1 shows the evaluation results for the nominal datasets (i.e., there is no misbehavior) from Circuit-1 and Circuit-2. With our chosen threshold, for MARMOT, we observe three FPs for MR5 (Horizontal Flip) in Circuit-2, which corresponds with a FPR (to be minimized) of 10%. For all other cases, we observe 0 FPs for all of MARMOT's MRs.

Table 2 shows the evaluation results for the anomaly datasets.. In terms of TPR (the higher, the better), we observe that MR5 achieves the best results in both circuits, 35% for Circuit-1 and 65% for Circuit-2. In comparison, the rest of the MRs achieve significantly lower TPR and F1 measures, indicating a much lower ability to identify external uncertainties. On the other hand, Table 3 shows the evaluation results for the mutant datasets (i.e., faults of the DNN based on the three chosen mutation operators from [22]). In this case, we observe that all of MARMOT's MRs achieve very high TPR and F1 scores, with TPRs higher than 77% in all cases. Furthermore, MR5 achieves 100% TPR in both circuits.

Table 1. Evaluation results for all oracles with Nominal datasets and a 10% threshold (average of 10 for SelfOracle), false positives in boldface.

| | Nominal | | | | | |
|------------------------|------------|------|------|------------|------|------|
| | Circuit-1 | | | Circuit-2 | | |
| | FP | TN | FPR | FP | TN | FPR |
| MARMOT | | | | | | |
| MR1: Reduce Brightness | 0.0 | 30.0 | 0.00 | 0.0 | 30.0 | 0.00 |
| MR2: Increase Contrast | 0.0 | 30.0 | 0.00 | 0.0 | 30.0 | 0.00 |
| MR3: Add Noise | 0.0 | 30.0 | 0.00 | 0.0 | 30.0 | 0.00 |
| MR4: Blur | 0.0 | 30.0 | 0.00 | 0.0 | 30.0 | 0.00 |
| MR5: Horizontal Flip | 0.0 | 30.0 | 0.00 | 3.0 | 27.0 | 0.10 |
| SelfOracle | | | | | | |
| CAE | 0.0 | 30.0 | 0.00 | 0.1 | 29.9 | 0.00 |
| DAE | 0.0 | 30.0 | 0.00 | 0.0 | 30.0 | 0.00 |
| SAE | 0.0 | 30.0 | 0.00 | 0.0 | 30.0 | 0.00 |
| VAE | 0.0 | 30.0 | 0.00 | 0.0 | 30.0 | 0.00 |
| Ensemble | 2.0 | 28.0 | 0.07 | 1.0 | 29.0 | 0.03 |

Table 4 shows the threshold-independent measures of AUC-PRC and AUC-ROC for both the anomaly and mutant datasets. Based on these metrics, we observe that MR5 (Horizontal Flip) achieves the best results in all cases, with MR1 (Reduce Brightness) and MR3 (Add Noise) being the next best MRs.

The reason why the effectiveness of MARMOT is much lower for identifying external anomalies might be related with the length of the reaction period, i.e., the period between the beginning of the anomalous scenario until the moment where the vehicle goes out-of-bounds. We observed that most of the image filters we implemented for the anomalies dataset cause the vehicle to drive off the road fairly quickly, leaving a monitor with a very short period to react. Conversely, many of the mutant DNNs are capable of driving within bounds for longer periods of time, which gives the monitors a much longer time to react to the DNNs uncertain behavior. The estimated average reaction period for the anomalies datasets recordings is around 7 seconds for Circuit-1 and 5 seconds for Circuit-2, whereas the reaction periods for the mutants datasets are around 40 seconds for Circuit-1 and 20 seconds for Circuit-2.

Table 2. Evaluation results for all oracles with Anomaly datasets and a 10% threshold (average of 10 for SelfOracle), best results in boldface

| | Anomaly | | | | | | | | | |
|------------------------|-----------|------|-------------|-------|-------------|-----------|------|-------------|-------|-------------|
| | Circuit-1 | | | | | Circuit-2 | | | | |
| | TP | FN | TPR | Prec. | F1 | TP | FN | TPR | Prec. | F1 |
| MARMOT | | | | | | | | | | |
| MR1: Reduce Brightness | 8.0 | 44.0 | 0.15 | 1.00 | 0.27 | 17.0 | 35.0 | 0.33 | 1.00 | 0.49 |
| MR2: Increase Contrast | 3.0 | 49.0 | 0.06 | 1.00 | 0.11 | 2.0 | 50.0 | 0.04 | 1.00 | 0.07 |
| MR3: Add Noise | 3.0 | 49.0 | 0.06 | 1.00 | 0.11 | 4.0 | 48.0 | 0.08 | 1.00 | 0.14 |
| MR4: Blur | 2.0 | 50.0 | 0.04 | 1.00 | 0.07 | 6.0 | 46.0 | 0.12 | 1.00 | 0.21 |
| MR5: Horizontal Flip | 18.0 | 34.0 | 0.35 | 1.00 | 0.51 | 34.0 | 18.0 | 0.65 | 0.92 | 0.76 |
| SelfOracle | | | | | | | | | | |
| CAE | 8.7 | 43.3 | 0.17 | 1.00 | 0.29 | 14.2 | 37.8 | 0.27 | 0.99 | 0.41 |
| DAE | 0.0 | 52.0 | 0.00 | 0.00 | 0.00 | 0.0 | 52.0 | 0.00 | 0.00 | 0.00 |
| SAE | 2.5 | 49.5 | 0.05 | 0.50 | 0.09 | 3.0 | 49.0 | 0.06 | 0.50 | 0.10 |
| VAE | 4.9 | 47.1 | 0.09 | 1.00 | 0.17 | 5.2 | 46.8 | 0.10 | 1.00 | 0.18 |
| Ensemble | 16.0 | 36.0 | 0.31 | 0.89 | 0.46 | 19.0 | 33.0 | 0.37 | 0.95 | 0.53 |

Table 3. Evaluation results for all oracles with Mutant datasets and a 10% threshold (average of 10 for SelfOracle), best results in boldface

| | Mutant | | | | | | | | | |
|------------------------|-----------|------|-------------|-------|-------------|-----------|------|-------------|-------|-------------|
| | Circuit-1 | | | | | Circuit-2 | | | | |
| | TP | FN | TPR | Prec. | F1 | TP | FN | TPR | Prec. | F1 |
| MARMOT | | | | | | | | | | |
| MR1: Reduce Brightness | 25.0 | 5.0 | 0.83 | 1.00 | 0.91 | 25.0 | 5.0 | 0.83 | 1.00 | 0.91 |
| MR2: Increase Contrast | 23.0 | 7.0 | 0.77 | 1.00 | 0.87 | 23.0 | 7.0 | 0.77 | 1.00 | 0.87 |
| MR3: Add Noise | 25.0 | 5.0 | 0.83 | 1.00 | 0.91 | 25.0 | 5.0 | 0.83 | 1.00 | 0.91 |
| MR4: Blur | 25.0 | 5.0 | 0.83 | 1.00 | 0.91 | 25.0 | 5.0 | 0.83 | 1.00 | 0.91 |
| MR5: Horizontal Flip | 30.0 | 0.0 | 1.00 | 1.00 | 1.00 | 30.0 | 0.0 | 1.00 | 0.91 | 0.96 |
| SelfOracle | | | | | | | | | | |
| CAE | 3.7 | 26.3 | 0.12 | 0.70 | 0.20 | 2.8 | 27.2 | 0.09 | 0.79 | 0.16 |
| DAE | 0.0 | 30.0 | 0.00 | 0.00 | 0.00 | 0.0 | 30.0 | 0.00 | 0.00 | 0.00 |
| SAE | 0.0 | 30.0 | 0.00 | 0.00 | 0.00 | 0.0 | 30.0 | 0.00 | 0.00 | 0.00 |
| VAE | 0.0 | 30.0 | 0.00 | 0.00 | 0.00 | 0.0 | 30.0 | 0.00 | 0.00 | 0.00 |
| Ensemble | 16.0 | 14.0 | 0.53 | 0.89 | 0.67 | 10.0 | 20.0 | 0.33 | 0.91 | 0.49 |

RQ1: In summary, we can conclude that MARMOT is very effective at identifying mutants, with TPRs ranging from 77% to 100%, while also being fairly effective at identifying external anomalies with at least one MR, with the TPRs for the best MR (Horizontal Flip) ranging from 35% to 65%.

4.6.2 RQ2 – Comparison. Table 1 shows that all oracles but Ensemble achieve 0 FPs for Circuit-1, whereas for Circuit-2, Ensemble, CAE (SelfOracle) and MR5 (Horizontal Flip) are the only oracles with FPs. Overall, the FPR (to be minimized) is not higher than 10% for any of the oracles, but the highest FPR is obtained by MARMOT’s MR5 in Circuit-2.

Table 2 shows that, in terms of TPR and F1 (to be maximized), MR5 achieves the best results in both circuits, followed by Ensemble, and then either MR1 (Reduce Brightness) or SelfOracle with the CAE model. On the other hand, we observe from Table 3 that all of MARMOT’s MRs achieve a significantly higher TPR and F1 score than the other approaches, followed by Ensemble. Here,

Table 4. Evaluation AUC results for all oracles and datasets (average of 10 for SelfOracle), best results in boldface

| | Anomaly | | | | Mutant | | | |
|------------------------|--------------|--------------|--------------|--------------|--------------|--------------|--------------|--------------|
| | Circuit-1 | | Circuit-2 | | Circuit-1 | | Circuit-2 | |
| | AUC-PRC | AUC-ROC | AUC-PRC | AUC-ROC | AUC-PRC | AUC-ROC | AUC-PRC | AUC-ROC |
| MARMOT | | | | | | | | |
| MR1: Reduce Brightness | 0.688 | 0.439 | 0.831 | 0.727 | 0.791 | 0.833 | 0.791 | 0.833 |
| MR2: Increase Contrast | 0.500 | 0.248 | 0.799 | 0.699 | 0.771 | 0.811 | 0.791 | 0.833 |
| MR3: Add Noise | 0.578 | 0.346 | 0.870 | 0.821 | 0.791 | 0.833 | 0.791 | 0.833 |
| MR4: Blur | 0.605 | 0.392 | 0.821 | 0.775 | 0.791 | 0.833 | 0.782 | 0.833 |
| MR5: Horizontal Flip | 0.751 | 0.546 | 0.841 | 0.776 | 0.958 | 1.000 | 0.958 | 1.000 |
| SelfOracle | | | | | | | | |
| CAE | 0.731 | 0.539 | 0.717 | 0.489 | 0.765 | 0.719 | 0.480 | 0.330 |
| DAE | 0.517 | 0.214 | 0.568 | 0.322 | 0.376 | 0.269 | 0.307 | 0.146 |
| SAE | 0.519 | 0.220 | 0.602 | 0.388 | 0.372 | 0.284 | 0.349 | 0.205 |
| VAE | 0.532 | 0.256 | 0.685 | 0.522 | 0.512 | 0.393 | 0.440 | 0.311 |
| Ensemble | 0.695 | 0.462 | 0.882 | 0.848 | 0.692 | 0.715 | 0.696 | 0.748 |

SelfOracle achieves TPRs of 12% or lower with CAE in both circuits, and 0% scores with the other autoencoder models.

Based on the threshold-independent measures from Table 4, we observe that all of MARMOT's MRs outperform both SelfOracle and Ensemble baselines by a significant margin for the mutant datasets. As for the anomalies, MR5 achieves the highest scores in Circuit-1, closely followed by SelfOracle's CAE model, and then followed by Ensemble. Surprisingly, Ensemble achieves the highest scores for the Circuit-2 anomalies, followed by MARMOT's MRs, and then followed by SelfOracle's CAE.

It is interesting that SelfOracle's CAE model achieves the best results among the four autoencoder models in our evaluation, whereas in the evaluation from Stocco et al. it obtained the worst results [42]. The relative ordering for the rest of the autoencoders from best to worst, is VAE, SAE, and lastly DAE, which does match the results obtained by Stocco et al. [42]. It is important to note that our dataset comprises pictures from a physical environment, whereas SelfOracle's original evaluation employed images obtained from a simulator. CAE's image reconstruction process appears to be more sensitive to anomalies in real images than the rest of the autoencoders, but less so in images generated from a simulator, which are generally simpler and contain fewer details.

Comparing the results from Circuit-1 and Circuit-2 for the anomalies datasets, we observe that all monitors obtained noticeably better results in Circuit-2, despite the fact that the reaction period for this circuit is slightly shorter on average (~7 seconds for Circuit-1 and ~5 seconds for Circuit-2). We speculate that the extra environmental uncertainties introduced in Circuit-2 (i.e., the discontinuous road boundaries and the extra line in the middle of the road) causes a slightly more erratic driving, which might make the uncertain behavior from anomalies to become more noticeable for the monitors. The results from Table 4 seem to indicate that Ensemble is the most favored by this factor. This may be due to the fact that Ensemble is a white-box approach, and thus potentially more sensitive to the DNNs internal erratic behavior than MARMOT and SelfOracle, which are black-box.

RQ2: In summary, we can conclude that MARMOT clearly outperforms both baselines in terms of identifying mutants, while also achieving a comparable or higher effectiveness at identifying external anomalies with the best MRs.

4.6.3 RQ3 – Reaction. In this RQ, we aim to account for the latency of the anomaly detection and reaction process that would exist in practice (communications latency, processing time, etc.), which

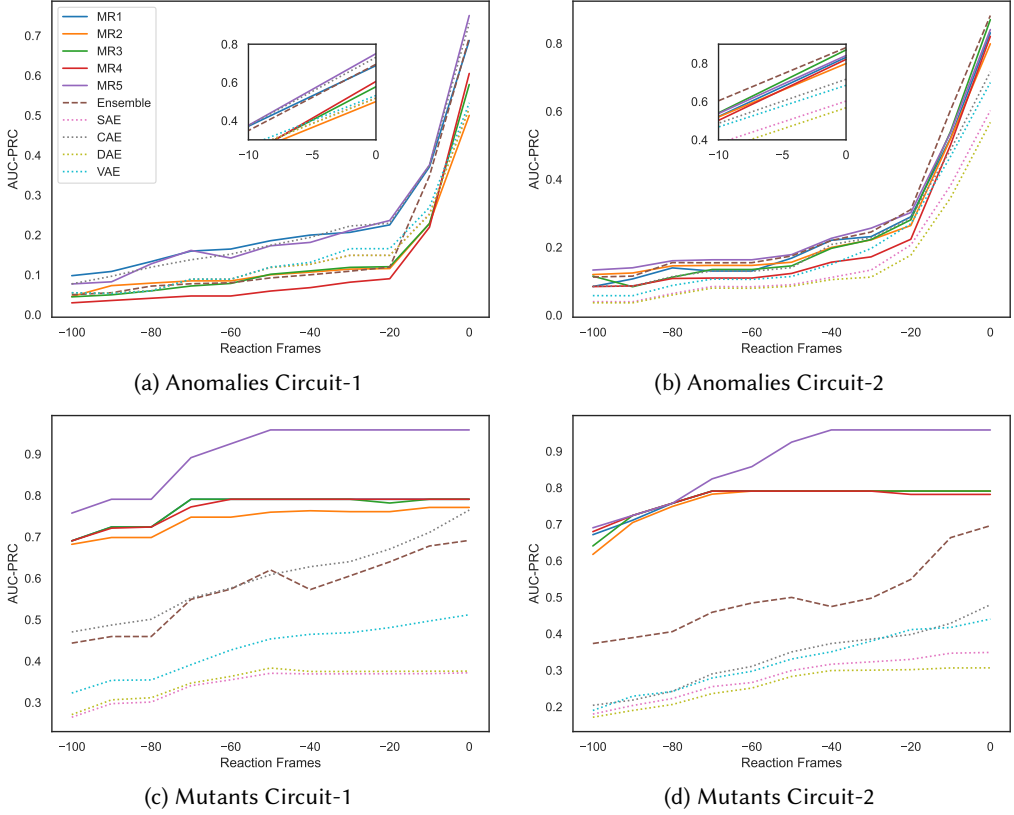


Fig. 4. AUC-PRC over reaction time

might prevent the triggered healing process (e.g., stopping the vehicle before out-of-bounds) from taking effect in time.

Figure 4 shows graphs with the different AUC-PRC scores (vertical axis) that would be obtained if we require the oracles to raise an alarm a certain amount of frames *before* the out-of-bounds happens (horizontal axis). For instance, the AUC-PRC at Reaction Frames = -20 is the measure that we would obtain in practice if we accounted for a delay of 20 frames from the moment an image is recorded until the oracle has processed it, the alarm is raised, and the healing action is taken. Since we process images at 10 FPSs, Reaction Frames = -20 corresponds with roughly two seconds of latency. Note that the rightmost values (Reaction Frames = 0) correspond with the measures from Table 4.

Figures 4a and 4b show the AUC-PRC scores for the external anomalies in Circuit-1 and Circuit-2 respectively. We can observe that the performance of all approaches degrades very significantly if we account for 10 or 20 latency frames. In practice, this might mean that achieving results similar to the ones presented in the previous RQs may require very low latency communications and processing. Nevertheless, MARMot and all the baselines seem to be affected by this in a very similar manner. The cause is likely to be the short reaction time between the moment the external anomaly happens and the out-of-bounds episode, as mentioned in the previous RQs.

On the other hand, Figures 4c and 4d show the AUC-PRC scores for the mutants in Circuit-1 and Circuit-2 respectively. In this case, we can see that MARMot's performance is almost completely

unaffected even if we account for up to 40 frames (around four seconds) of latency. This should be realistically more than enough reaction time even if MARMOT's processing is performed in a separate computational unit communicating with the LeoRover. On the other hand, both baselines show a steady degradation in their effectiveness if any amount of latency is accounted for. Since SelfOracle derives its uncertainty scores purely from the DNN inputs (i.e., the camera images), it makes sense that most uncertain behaviors are identified shortly before the out-of-bounds occurs, which causes its efficiency to degrade if we account for some latency. Conversely, MARMOT does consider the DNN output, which can make it more sensitive to the DNN's internal behavior and allow it to identify mutants early. Despite being a white-box approach, Ensemble does not seem to identify uncertain behaviors until shortly before the out-of-bounds occurs, as the graphs show a steady degradation of AUC-PRC comparable with SelfOracle's.

RQ3: In summary, we conclude that in the case of anomalies, the performance of MARMOT and both baselines degrades significantly if we account for a small latency. Conversely, in the case of mutants, the performance of MARMOT remains identical even with a latency of up to four seconds.

4.7 Threats to Validity

We now discuss the main threats of our evaluation and how we tried to mitigate them.

4.7.1 Internal validity. The generated mutants and anomalies suppose potential internal validity threats in our study. For the mutants, we mitigated them by using some of the mutation operators recommended by Humatova et al. [22]. As for the anomalies, we used the image corruptions and perturbations proposed by [19], which are widely used for testing image-based DNNs. The employed DNN architecture and its training configuration could be another internal validity threat. We mitigated it by employing the same architecture as suggested by the manufacturer. Moreover, we used the same architecture and parameters for the baseline of SelfOracle as its original paper [42]. The selected MRs 1 to 4 have some parameters (e.g., brightness level). Different parameters may lead to different results. To mitigate this threat, we verify that our parameters will result in valid follow-up inputs. We follow the definition provided by [35] to define a valid test input in the domain of DNN-based autonomous driving systems, i.e., the image is recognizable by a human expert.

4.7.2 External validity. We employed a single case study system, which poses a threat in terms of generalizability. We mitigated this threat by employing two different circuits, different anomaly types and different DNN mutants, resulting in a diverse dataset. Moreover, the employed case study system was a physical one, which reduces the threat posed by the gap between simulators and real ADSs.

4.7.3 Conclusion validity. The employed baseline, i.e., SelfOracle [42], employs neural networks, and as such, the training process is stochastic. To reduce the threat that the obtained results are by chance, we train each configuration of SelfOracle 10 times and provide average values in the evaluation.

5 RELATED WORK

Automated test generation techniques have been the most widely investigated technique to identify unexpected driving scenarios of ADSs. This has been targeted from different perspectives, including techniques to maximize neuron coverage [34], surrogate-assisted search-based test generation [1, 2, 17, 31], techniques based on reinforcement learning [18, 30] and procedural content generation to generate virtual roads [15]. These studies focus on detecting unexpected scenarios at design-time,

before deploying the system in operation. Conversely, our approach focuses on proposing a run-time monitoring technique to build a safety envelope over a DNN to assess its level of dependability in operation.

In this context, i.e., run-time monitoring of DNN-enabled ADSs, black-box [42, 42] and white-box [39] approaches have been recently proposed, as discussed throughout the paper. Our approach falls in the scope of the black-box ones. In such an scope, frameworks such as SelfOracle [42] and DeepGuard [23] train auto-encoders with the same images used for training the ADS, and use the reconstruction error of these auto-encoders as an uncertainty score. Unlike existing black-box approaches, MARMOT does not require any training, as it relies on metamorphic relations to generate follow-up inputs and subsequently obtain a confidence score through output relations. Moreover, MARMOT overcomes the limitation identified by Stocco et al. [39] for black-box techniques, i.e., failing to detect faults caused by an inadequate training or by bugs at the DNN model level, as we demonstrated in our evaluation.

Our approach is largely inspired by Metamorphic Testing, a technique that has been found effective at alleviating the test oracle problem [38]. This technique has also been explored in the context of ADSs [11, 12, 38, 44, 50, 53]. Tian et al. [44] proposed DeepTest, a testing framework to identify erroneous behaviors of DNN-based self-driving cars through MR-based test oracles. Zhang et al. [50] proposed DeepRoad, an ADS testing framework that leverages Generative Adversarial Networks (GANs) to automatically generate realistic follow-up images simulating various weather conditions, such as snow or rain. Deng et al. [11] propose a Behaviour-Driven Development (BDD) workflow in which MRs are expressed in a declarative manner by the test engineers. The framework converts declared MRs to executable oracles in addition to the synthesis of test inputs for each MR [11]. The same team later proposed a rule-based declarative framework that leverages natural language processing (NLP) to extract MRs from predicates written in natural language [12]. Unlike all these studies, which focus on design-time testing of ADSs, our approach leverages MRs for operational purposes with the goal of detecting potential misbehaviors and take corresponding healing actions in run-time.

To the best of our knowledge, there are only three papers that have proposed the use of MT at run-time [5, 32, 33]. These papers introduce the concept of *Metamorphic Runtime Checking*, which is the analogous of runtime assertion checking for MRs [5]. Similar to our work, their approach also involves intercepting inputs at runtime and executing follow-up test inputs to check MRs. In contrast to our work, which aims to monitor ADSs, they apply this technique to monitor generic software applications [33] and their individual functions [5, 32]. Their approach involves creating a “sandbox” in order to execute the follow-up test cases, which typically involves forking the process, in order to ensure identical state from the original execution [5]. This sandboxing process is unnecessary for MARMOT, since DNNs are generally isolated components which do not depend on external state. Given the application domain, the monitors they generate employ assertions (pass or fail). Unlike these approaches, we leverage metamorphic relations with the goal of measuring the uncertainty of the ADS controller in an efficient and effective way. MARMOT later employs these quantitative uncertainty scores in an auto-regressive filter to consider past values and raise a flag in case this value exceeds a predefined threshold. To the best of our knowledge, this paper is the first that aims at adapting MT to run-time monitoring in a context of AVs and CPSs.

6 CONCLUSION

We propose MARMOT, a novel run-time monitoring approach that leverages ideas from Metamorphic Testing to estimate the confidence of ADS controllers. Our evaluation, which uses a small-scale ADS, shows that MARMOT is capable of effectively anticipating failures caused by either internal or external uncertainties before the vehicle goes out-of-bounds. Indeed, our approach outperformed

or at least showed the same performance as the employed baselines (i.e., SelfOracle [42] and Ensemble-based techniques).

Future work includes comparing our approach with other confidence estimators, such as those based on eXplainable AI (XAI) techniques. Furthermore, we also plan to evaluate the impact of combining these techniques with different self-healing mechanisms, such as slowing down the vehicle when facing a sudden peak of the uncertainty score.

REPLICATION PACKAGES:

We make all our artifacts available as follows:

- Our dataset can be found at: <https://doi.org/10.5281/zenodo.8202317>
- Our code is available at: <https://github.com/jonayerdi/marmot>

ACKNOWLEDGMENTS

This work was partially founded by the Basque Government through their Elkartek program (EGIA project, ref. KK-2022/00119 and SIIRSE project, ref. KK-2022/00007). The authors are part of the Software and Systems Engineering research group of Mondragon Unibertsitatea (IT1519-22), supported by the Department of Education, Universities and Research of the Basque Country.

REFERENCES

- [1] Raja Ben Abdesslem, Shiva Nejati, Lionel C Briand, and Thomas Stifter. 2018. Testing vision-based control systems using learnable evolutionary algorithms. In *Proceedings of the 40th International Conference on Software Engineering*. 1016–1026.
- [2] Raja Ben Abdesslem, Annibale Panichella, Shiva Nejati, Lionel C Briand, and Thomas Stifter. 2018. Testing autonomous cars for feature interaction failures using many-objective search. In *Proceedings of the 33rd ACM/IEEE International Conference on Automated Software Engineering*. 143–154.
- [3] Apollo. 2023. Apollo Website. <https://developer.apollo.auto/index.html> Accessed: August 1, 2023.
- [4] Jon Ayerdi, Pablo Valle, Asier Iriarte, Ibai Roman, Miren Illarramendi, and Aitor Arrieta. 2023. *Dataset for "MarMot: Metamorphic Runtime Monitoring of Autonomous Driving Systems"*. <https://doi.org/10.5281/zenodo.8202317>
- [5] Jonathan Bell, Christian Murphy, and Gail Kaiser. 2015. Metamorphic runtime checking of applications without test oracles. *CrossTalk* 28, 2 (2015).
- [6] Raja Ben Abdesslem, Shiva Nejati, Lionel C Briand, and Thomas Stifter. 2016. Testing advanced driver assistance systems using multi-objective search and neural networks. In *Proceedings of the 31st IEEE/ACM international conference on automated software engineering*. 63–74.
- [7] Matteo Biagiola and Paolo Tonella. 2022. Testing the plasticity of reinforcement learning-based systems. *ACM Transactions on Software Engineering and Methodology (TOSEM)* 31, 4 (2022), 1–46.
- [8] Mariusz Bojarski, Davide Del Testa, Daniel Dworakowski, Bernhard Firner, Beat Flepp, Prasoon Goyal, Lawrence D Jackel, Mathew Monfort, Urs Muller, Jiakai Zhang, et al. 2016. End to end learning for self-driving cars. *arXiv preprint arXiv:1604.07316* (2016).
- [9] Alessandro Calò, Paolo Arcaini, Shaikat Ali, Florian Hauer, and Fuyuki Ishikawa. 2020. Generating avoidable collision scenarios for testing autonomous driving systems. In *2020 IEEE 13th International Conference on Software Testing, Validation and Verification (ICST)*. IEEE, 375–386.
- [10] T. Y. Chen, S. C. Cheung, and S. M. Yiu. 1998. *Metamorphic Testing: A New Approach for Generating Next Test Cases*. Technical Report. Technical Report HKUST-CS98-01, Department of Computer Science, The Hong Kong University of Science and Technology.
- [11] Yao Deng, Guannan Lou, Xi Zheng, Tianyi Zhang, Miryung Kim, Huai Liu, Chen Wang, and Tsong Yueh Chen. 2021. BMT: Behavior driven development-based metamorphic testing for autonomous driving models. In *2021 IEEE/ACM 6th International Workshop on Metamorphic Testing (MET)*. IEEE, 32–36.
- [12] Yao Deng, Xi Zheng, Tianyi Zhang, Huai Liu, Guannan Lou, Miryung Kim, and Tsong Yueh Chen. 2022. A declarative metamorphic testing framework for autonomous driving. *IEEE Transactions on Software Engineering* (2022).
- [13] Raul Sena Ferreira, Jean Arlat, Jérémie Guiochet, and Hélène Waeselynck. 2021. Benchmarking safety monitors for image classifiers with machine learning. In *2021 IEEE 26th Pacific Rim International Symposium on Dependable Computing (PRDC)*. IEEE, 7–16.

- [14] Alessio Gambi, Tri Huynh, and Gordon Fraser. 2019. Generating effective test cases for self-driving cars from police reports. In *Proceedings of the 2019 27th ACM Joint Meeting on European Software Engineering Conference and Symposium on the Foundations of Software Engineering*. 257–267.
- [15] Alessio Gambi, Marc Mueller, and Gordon Fraser. 2019. Automatically testing self-driving cars with search-based procedural content generation. In *Proceedings of the 28th ACM SIGSOFT International Symposium on Software Testing and Analysis*. 318–328.
- [16] Joris Guerin, Kevin Delmas, and Jérémie Guiochet. 2022. Evaluation of runtime monitoring for UAV emergency landing. In *2022 International Conference on Robotics and Automation (ICRA)*. IEEE, 9703–9709.
- [17] Fitash Ul Haq, Donghwan Shin, and Lionel Briand. 2022. Efficient online testing for DNN-enabled systems using surrogate-assisted and many-objective optimization. In *Proceedings of the 44th international conference on software engineering*. 811–822.
- [18] Fitash Ul Haq, Donghwan Shin, and Lionel C Briand. 2023. Many-objective reinforcement learning for online testing of dnn-enabled systems. In *2023 IEEE/ACM 45th International Conference on Software Engineering (ICSE)*. IEEE, 1814–1826.
- [19] Dan Hendrycks and Thomas Dietterich. 2019. Benchmarking Neural Network Robustness to Common Corruptions and Perturbations. *Proceedings of the International Conference on Learning Representations* (2019).
- [20] Jens Henriksson, Christian Berger, Markus Borg, Lars Tornberg, Cristofer Englund, Sankar Raman Sathyamoorthy, and Stig Ursing. 2019. Towards structured evaluation of deep neural network supervisors. In *2019 IEEE International Conference On Artificial Intelligence Testing (AITest)*. IEEE, 27–34.
- [21] Nargiz Humbatova, Gunel Jahangirova, Gabriele Bavota, Vincenzo Riccio, Andrea Stocco, and Paolo Tonella. 2020. Taxonomy of real faults in deep learning systems. In *Proceedings of the ACM/IEEE 42nd International Conference on Software Engineering*. 1110–1121.
- [22] Nargiz Humbatova, Gunel Jahangirova, and Paolo Tonella. 2021. Deepcrime: mutation testing of deep learning systems based on real faults. In *Proceedings of the 30th ACM SIGSOFT International Symposium on Software Testing and Analysis*. 67–78.
- [23] Manzoor Hussain, Nazakat Ali, and Jang-Eui Hong. 2022. DeepGuard: a framework for safeguarding autonomous driving systems from inconsistent behaviour. *Automated Software Engineering* 29, 1 (2022), 1.
- [24] Jinhan Kim, Robert Feldt, and Shin Yoo. 2019. Guiding deep learning system testing using surprise adequacy. In *2019 IEEE/ACM 41st International Conference on Software Engineering (ICSE)*. IEEE, 1039–1049.
- [25] Anis Koubâa et al. 2017. *Robot Operating System (ROS)*. Vol. 1. Springer.
- [26] Balaji Lakshminarayanan, Alexander Pritzel, and Charles Blundell. 2017. Simple and Scalable Predictive Uncertainty Estimation using Deep Ensembles. In *Advances in Neural Information Processing Systems*, I. Guyon, U. Von Luxburg, S. Bengio, H. Wallach, R. Fergus, S. Vishwanathan, and R. Garnett (Eds.), Vol. 30. Curran Associates, Inc. https://proceedings.neurips.cc/paper_files/paper/2017/file/9ef2ed4b7fd2c810847ffa5fa85bce38-Paper.pdf
- [27] LeoRover. 2022. LeoRover Dataset. <https://www.kaggle.com/datasets/aleksanderszymaski/full-track>. Accessed on Jul 30, 2023.
- [28] LeoRover. 2023. LeoRover. <https://github.com/LeoRover>. Accessed on Jul 30, 2023.
- [29] Mikael Lindvall, Adam Porter, Gudjon Magnusson, and Christoph Schulze. 2017. Metamorphic model-based testing of autonomous systems. In *2017 IEEE/ACM 2nd International Workshop on Metamorphic Testing (MET)*. IEEE, 35–41.
- [30] Chengjie Lu, Yize Shi, Huihui Zhang, Man Zhang, Tiexin Wang, Tao Yue, and Shaukat Ali. 2022. Learning configurations of operating environment of autonomous vehicles to maximize their collisions. *IEEE Transactions on Software Engineering* 49, 1 (2022), 384–402.
- [31] Galen E Mullins, Paul G Stankiewicz, R Chad Hawthorne, and Satyandra K Gupta. 2018. Adaptive generation of challenging scenarios for testing and evaluation of autonomous vehicles. *Journal of Systems and Software* 137 (2018), 197–215.
- [32] Christian Murphy and Gail E Kaiser. 2009. Metamorphic runtime checking of non-testable programs. (2009).
- [33] Christian Murphy, Kuang Shen, and Gail Kaiser. 2009. Automatic system testing of programs without test oracles. In *Proceedings of the eighteenth international symposium on Software testing and analysis*. 189–200.
- [34] Kexin Pei, Yinzhi Cao, Junfeng Yang, and Suman Jana. 2017. Deepxplore: Automated whitebox testing of deep learning systems. In *proceedings of the 26th Symposium on Operating Systems Principles*. 1–18.
- [35] Vincenzo Riccio and Paolo Tonella. 2023. When and Why Test Generators for Deep Learning Produce Invalid Inputs: an Empirical Study. In *2023 IEEE/ACM 45th International Conference on Software Engineering (ICSE)*. IEEE, 1161–1173.
- [36] Lukas Ruff, Jacob R Kauffmann, Robert A Vandermeulen, Grégoire Montavon, Wojciech Samek, Marius Kloft, Thomas G Dietterich, and Klaus-Robert Müller. 2021. A unifying review of deep and shallow anomaly detection. *Proc. IEEE* 109, 5 (2021), 756–795.
- [37] Franz Scheuer, Alessio Gambi, and Paolo Arcaini. 2023. STRETCH: Generating Challenging Scenarios for Testing Collision Avoidance Systems. In *2023 IEEE Intelligent Vehicles Symposium (IV)*. IEEE, 1–6.

- [38] Sergio Segura, Gordon Fraser, Ana B Sanchez, and Antonio Ruiz-Cortés. 2016. A survey on metamorphic testing. *IEEE Transactions on software engineering* 42, 9 (2016), 805–824.
- [39] Andrea Stocco, Paulo J Nunes, Marcelo D’Amorim, and Paolo Tonella. 2022. Thirdeye: Attention maps for safe autonomous driving systems. In *Proceedings of the 37th IEEE/ACM International Conference on Automated Software Engineering*. 1–12.
- [40] Andrea Stocco, Brian Pulfer, and Paolo Tonella. 2022. Mind the gap! a study on the transferability of virtual vs physical-world testing of autonomous driving systems. *IEEE Transactions on Software Engineering* (2022).
- [41] Andrea Stocco and Paolo Tonella. 2022. Confidence-driven weighted retraining for predicting safety-critical failures in autonomous driving systems. *Journal of Software: Evolution and Process* 34, 10 (2022), e2386.
- [42] Andrea Stocco, Michael Weiss, Marco Calzana, and Paolo Tonella. 2020. Misbehaviour prediction for autonomous driving systems. In *Proceedings of the ACM/IEEE 42nd international conference on software engineering*. 359–371.
- [43] Yang Sun, Christopher M Poskitt, Jun Sun, Yuqi Chen, and Zijiang Yang. 2022. LawBreaker: An approach for specifying traffic laws and fuzzing autonomous vehicles. In *Proceedings of the 37th IEEE/ACM International Conference on Automated Software Engineering*. 1–12.
- [44] Yuchi Tian, Kexin Pei, Suman Jana, and Baishakhi Ray. 2018. Deeptest: Automated testing of deep-neural-network-driven autonomous cars. In *Proceedings of the 40th international conference on software engineering*. 303–314.
- [45] Huiyan Wang, Jingwei Xu, Chang Xu, Xiaoxing Ma, and Jian Lu. 2020. Dissector: Input validation for deep learning applications by crossing-layer dissection. In *Proceedings of the ACM/IEEE 42nd International Conference on Software Engineering*. 727–738.
- [46] Michael Weiss and Paolo Tonella. 2023. Uncertainty quantification for deep neural networks: An empirical comparison and usage guidelines. *Software Testing, Verification and Reliability* (2023).
- [47] Yan Xiao, Ivan Beschastnikh, David S Rosenblum, Changsheng Sun, Sebastian Elbaum, Yun Lin, and Jin Song Dong. 2021. Self-checking deep neural networks in deployment. In *2021 IEEE/ACM 43rd International Conference on Software Engineering (ICSE)*. IEEE, 372–384.
- [48] Man Zhang, Shaukat Ali, Tao Yue, Roland Norgren, and Oscar Okariz. 2019. Uncertainty-wise cyber-physical system test modeling. *Software & Systems Modeling* 18 (2019), 1379–1418.
- [49] Man Zhang, Bran Selic, Shaukat Ali, Tao Yue, Oscar Okariz, and Roland Norgren. 2016. Understanding uncertainty in cyber-physical systems: a conceptual model. In *Modelling Foundations and Applications: 12th European Conference, ECMFA 2016, Held as Part of STAF 2016, Vienna, Austria, July 6-7, 2016, Proceedings 12*. Springer, 247–264.
- [50] Mengshi Zhang, Yuqun Zhang, Lingming Zhang, Cong Liu, and Sarfraz Khurshid. 2018. DeepRoad: GAN-based metamorphic testing and input validation framework for autonomous driving systems. In *Proceedings of the 33rd ACM/IEEE International Conference on Automated Software Engineering*. 132–142.
- [51] Ziyuan Zhong, Gail Kaiser, and Baishakhi Ray. 2022. Neural network guided evolutionary fuzzing for finding traffic violations of autonomous vehicles. *IEEE Transactions on Software Engineering* (2022).
- [52] Yuan Zhou, Yang Sun, Yun Tang, Yuqi Chen, Jun Sun, Christopher M Poskitt, Yang Liu, and Zijiang Yang. 2023. Specification-based Autonomous Driving System Testing. *IEEE Transactions on Software Engineering* (2023).
- [53] Zhi Quan Zhou and Liqun Sun. 2019. Metamorphic testing of driverless cars. *Commun. ACM* 62, 3 (2019), 61–67.